Journal of Geophysical Research: Oceans

RESEARCH ARTICLE
10.1029/2018JC014110

Key Points:
- Nitrate isotope ratios evidence a highly regenerated nitrate reservoir in the halocline, originating from the Chukchi shelf
- Coupled nitrification-denitrification in shelf sediments transmits a large N deficit and elevated nitrate N isotope ratios to the halocline
- The nitrate reservoir in Atlantic Water derives from distinct inflows at Fram Strait

Supporting Information:
- Supporting Information S1

Correspondence to:
J. Granger,
julie.granger@uconn.edu

Citation:
Granger, J., Sigman, D. M., Gagnon, J., Tremblay, J.-E., & Mucci, A. (2018). On the properties of the Arctic halocline and deep water masses of the Canada Basin from nitrate isotope ratios. *Journal of Geophysical Research: Oceans*, *123*, 5443–5458. https://doi.org/10.1029/2018JC014110

Received 24 APR 2018
Accepted 7 JUL 2018
Accepted article online 17 JUL 2018
Corrected 20 AUG 2018
Published online 10 AUG 2018

This article was corrected on 20 AUG 2018. See the end of the full text for details.

On the Properties of the Arctic Halocline and Deep Water Masses of the Canada Basin from Nitrate Isotope Ratios

Julie Granger[1], Daniel M. Sigman[2], Jonathan Gagnon[3], Jean-Eric Tremblay[3], and Alfonso Mucci[4]

[1]Department of Marine Sciences, University of Connecticut, Storrs, CT, USA, [2]Geosciences Department, Princeton University, Princeton, NJ, USA, [3]Département de Biologie et Québec-Océan, Université Laval, Quebec, QC, Canada, [4]GEOTOP and Department of Earth and Planetary Sciences, McGill University, Montreal, QC, Canada

Abstract Nitrogen is a limiting nutrient for primary production in the western Arctic Ocean. Measurements of the nitrogen ($^{15}N/^{14}N$) and oxygen ($^{18}O/^{16}O$) isotope ratios of nitrate in the southeastern Beaufort Sea provide insight into biogeochemical cycling of nitrogen in the western Arctic Ocean. Nitrate O isotope ratios in the Pacific halocline evidence a highly regenerated reservoir. Coincident peaks in nutrient concentrations and reduced dissolved oxygen concentrations suggest that nitrate accrues from organic matter remineralization in bottom waters of the Chukchi shelf and that these ventilate the basin predominantly in summer, when isolated from the atmosphere. Preformed nitrate in Pacific Winter Water lacks $^{18}O/^{16}O$ elevation from nitrate assimilation, contrasting with preformed nitrate in other ocean regions. A reactive N deficit and elevated nitrate N isotope ratios in the Pacific halocline further indicate substantial N loss to coupled nitrification-denitrification in shelf sediments upstream. In the Atlantic Water below, nitrate isotope ratios identify two distinct waters entering the Arctic at Fram Strait, from (1) the surface West Spitsbergen Current, bearing isotopic signatures akin to North Atlantic waters, and (2) deeper inflows of waters ventilated in the Nordic Seas, transporting nitrate O isotope ratios indicative of regenerated nitrate. Poorly ventilated Canada Basin Deep Water shows evidence of nominal accrual of remineralized products, and nitrate isotope ratios suggest an influence of slow benthic denitrification on the sea floor. The observations reveal that shelf processes have a disproportionate influence on tracer properties of the Pacific halocline, while those in Atlantic Water are dominated by processes in the Nordic Seas.

1. Introduction

The Arctic Ocean is the world's smallest ocean, comprising only 4% of the global ocean area, and arguably the most distinct. It is largely enclosed by continents and is bordered by 20% of the world's continental shelves, which has led some oceanographers to refer to it as the Arctic Mediterranean (Aagaard et al., 1985; Rudels, 2010). It is filled by water from the Pacific via the Bering Strait and by water from the Atlantic via the Nordic Seas, also receiving significant input from rivers. The Arctic Ocean is salinity-stratified, composed of several vertical layers with prominent temperature inversions, as fresher Pacific-derived water overlies warmer and more saline Atlantic water (AW; see Timmermans et al., 2014). For much of the year, the Arctic shelves and basins are covered by ice, the concentrations and temporal dynamics of which modulate inherent hydrographic characteristics (e.g., Jackson et al., 2011).

The unique physical features of the Arctic Ocean influence the biogeochemistry and productivity of its shelf seas and basins. In the Western Arctic, the seasonal retreat of sea ice gives way to highly productive shelf blooms fueled by nutrient-rich Pacific waters entering through the Bering Strait (e.g., Wang et al., 2005). The remineralization of organic matter on the shallow shelves promotes sedimentary denitrification, which progressively depletes reactive nitrogen concentrations in overlying waters (Brown et al., 2015; Chang & Devol, 2009; Granger et al., 2011). Shelf waters ventilate the subsurface Pacific halocline of the Western Arctic basins, such that primary production upon ice retreat is ultimately limited by the supply of reactive nitrogen from the subsurface (Carmack et al., 2004; Le Fouest et al., 2013; Tremblay et al., 2015). In spite of the small areal extent of the Arctic Ocean, benthic N loss on the continental shelves represents an important global sink, accounting for 4% to 13% of the global oceanic reactive N loss (Chang & Devol, 2009). These phosphate-rich, N-depleted waters eventually reach the North Atlantic and are hypothesized to promote

N_2 fixation in North Atlantic basin (Yamamoto-Kawai et al., 2006). Deeper waters in the Canada Basin originate from the Nordic Seas, where biogeochemical cycling on the shelves and deep winter convection in the basins likely imprint the nutrient inventory.

The Arctic Ocean is undergoing rapid changes, having seen an ~1 °C increase in mean air temperature since the 1970s (Berner et al., 2005; IPCC, 2014) and a drop in the concentration, thickness, and seasonal duration of sea ice (Comiso, 2011; James et al., 2011; Perovich & Richter-Menge, 2009). In the Canada Basin, the surface mixed layer has freshened (McLaughlin et al., 2011; Morison et al., 2012; Serreze et al., 2006; Yamamoto-Kawai et al., 2009), warmed (Jackson et al., 2010), and shoaled, becoming increasingly stratified (McLaughlin & Carmack, 2010; Toole et al., 2010). The increase in the number of days of open water has lengthened the phytoplankton growing season (Arrigo et al., 2008), engendering a 20% increase in net primary production in shelf regions of the Arctic Ocean between 1998 and 2009 (Arrigo & Van Dijken, 2011).

With the release of phytoplankton from light limitation, fixed N availability will exert increasing influence on the fertility of the Arctic Ocean and the strength of its biological carbon pump. Regional changes in circulation are also likely to modulate N transports and cycling of the shelves and basins. These dynamics underscore the importance of understanding N cycling in the context of the current hydrography of the Arctic basins. To this end, the nitrogen ($^{15}N/^{14}N$) and oxygen ($^{16}O/^{18}O$) isotope ratios of nitrate (NO_3^-) provide integrative tracers with which to diagnose hydrographic transport and biogeochemical cycling. Henceforth, the isotope ratios are reported in delta notation (δ) in units of per mille (‰), where the $^{15}N/^{14}N$ reference is N_2 in air, and the $^{18}O/^{16}O$ reference is Vienna standard mean ocean water (VSMOW):

$$\delta^{15}N(‰) = \left[\left(\frac{^{15}N}{^{14}N_{sample}} \Big/ \frac{^{15}N}{^{14}N_{air}}\right) - 1\right] x\ 1000.$$

$$\delta^{18}O(‰) = \left[\left(\frac{^{18}O}{^{16}O_{sample}} \Big/ \frac{^{18}O}{^{16}O_{VSMOW}}\right) - 1\right] x\ 1000.$$

In general terms, the N and O isotopologues of NO_3^- record complementary biogeochemical processes. In the subsurface, NO_3^- is the dominant reservoir of reactive N, originating primarily from the remineralization of organic material exported from the sea surface. As such, the $\delta^{15}N$ of remineralized NO_3^- records that of reactive N assimilated at the sea surface, which derives from the $\delta^{15}N$ of upwelled NO_3^-, as well as the $\delta^{15}N$ of reactive N added by in situ biological N_2 fixation and exogenous sources such as atmospheric deposition and river discharge. The subsurface NO_3^- reservoir is further sensitive to water-column denitrification, which increases the $\delta^{15}N_{NO3}$ in proportion to N loss. Preformed NO_3^- (Redfield, 1958) can also contribute to subsurface NO_3^-. In the Pacific Ocean, for instance, the $\delta^{15}N$ of preformed NO_3^- is relatively ^{15}N-enriched due to partial NO_3^- assimilation at the surface of the Southern Ocean prior to the subduction in intermediate and mode waters (Rafter et al., 2013). In contrast to $\delta^{15}N_{NO3}$, the $\delta^{18}O$ of remineralized NO_3^- is characteristically close to that of water, such that it is insensitive to the origin of the remineralized organic N, facilitating its distinction from other inputs. Like $\delta^{15}N_{NO3}$, the $\delta^{18}O$ of the subsurface NO_3^- reservoir increases proportionally to N loss from water-column denitrification (Granger et al., 2008; Sigman et al., 2005), and the $\delta^{18}O$ of preformed NO_3^- can also be ^{18}O-enriched from partial NO_3^- assimilation at the sea surface (Rafter et al., 2013). Interpreted in tandem, the coupled $\delta^{15}N$ and $\delta^{18}O$ of NO_3^- provide complementary constraints on the N budget.

In order to develop a more robust understanding of the regional N inventory of the western Arctic Ocean, we present measurements of the N and O isotopic composition of NO_3^- in the southeastern Beaufort Sea undertaken as part of the Canada International Polar Year GEOTRACES effort. In combination with ancillary hydrographic and chemical tracers, the measurements provide biogeochemical insights into prominent hydrographic features, highlighting regional N transport and characterizing biological N transformations. The measurements also provide insights on the ventilation of subsurface water masses, from which to better contextualize N cycling in the changing Arctic.

2. Materials and Methods

Hydrographic stations spanning a meridional transect at 136°W from the continental slope to 75.3°N into the southern Beaufort Sea were visited aboard the icebreaker *CCGS Amundsen* as part of the Canada International

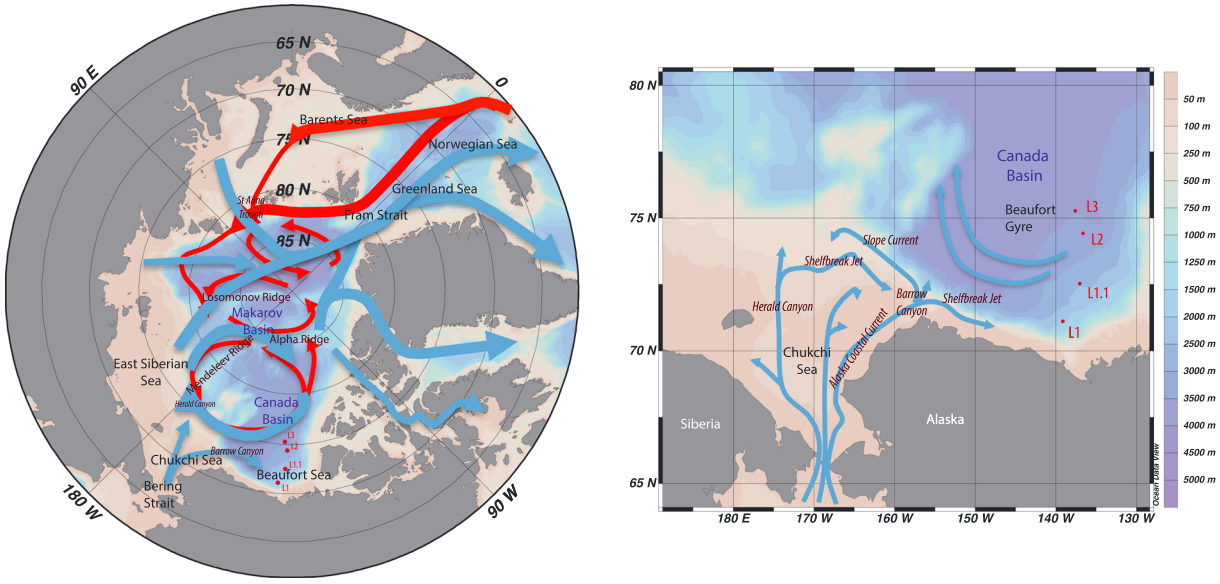

Figure 1. (a) Map of the Arctic Ocean with the location of hydrographic stations sampled in the southeastern Canada Basin, overlain with a schematic of dominant circulation pathways (reproduced from Pnyushkov et al., 2015). Blue arrows indicate surface circulation, and red arrows show the flow of Atlantic Water. Warm, saline Atlantic Water enters via the Barents Sea and through Fram Strait, following the Barents slope and around the Laptev Sea. A branch returns along the Losomonov Ridge, while another continues along the Siberian slope and around the Canada Basin. Remnant Atlantic water exits the Arctic via Fram Strait (not shown). Cold, fresher water from the Pacific enters at Bering Strait, draining into the Canada Basin at Herald and Barrow Canyons, joining the Beaufort Gyre. Surface waters exit through the Canadian Archipelago and at Fram Strait. (b) Schematic of the circulation of the Chukchi Sea and Beaufort Sea (reproduced from Corlett & Pickart, 2017). Maps were generated using ocean data view (Schlitzer, 2016).

Polar Year -GEOTRACES effort in August–September of 2009 (ArcticNet 0903; Figure 1a). In late summer of 2009, the shelf seas in our study area were ice-free, while the deep basin was covered by heterogeneous sea ice (Barber et al., 2009; Galley et al., 2013).

Seawater samples were collected at discrete depth intervals from the surface to the bottom using a tethered rosette holding twenty-four 12-L Niskin bottles for separate surface and deeper casts. Hydrographic measurements were made using a conductivity-temperature-depth profiler (CTD; Seabird® SBE 911plus). The temperature and conductivity probes were calibrated by the manufacturer, and a further calibration of the conductivity sensor was carried out using discrete salinity samples taken throughout the water column and analyzed on a Guildline Autosal 8400 salinometer calibrated with International Association for Physical Sciences of the Oceans standard seawater (practical salinity [S_P]). The CTD oxygen sensor (SBE-43) was calibrated against discrete seawater samples analyzed for dissolved oxygen concentration by Winkler titration (Carpenter, 1965; Grasshoff et al., 1983) with a reproducibility of 2 μmol/L.

Seawater samples for nutrient analyses and NO_3^- isotope analyses were filtered through a 0.2-μm pore-size polyethersulfone membrane into 60-ml high density polyethylene bottles and were stored frozen until analysis. Nutrients (NO_3^-, NO_2^-, soluble reactive phosphate [SRP], $Si(OH)_4$, and NH_4^+) were analyzed directly on board with a Technichon II autoanalyzer using standard methods (Gordon et al., 1992; Mantoura & Woodward, 1983). The naturally occurring isotope ratios of nitrogen ($^{15}N/^{14}N$) and oxygen ($^{18}O/^{16}O$) in nitrate (NO_3^-) were analyzed by the denitrifier method (Casciotti et al., 2002; Sigman et al., 2001). Briefly, 20 nmol of NO_3^- were quantitatively reduced to nitrous oxide (N_2O) gas by denitrifying bacteria that lack an active terminal N_2O reductase (*P. chlororaphis* f. sp. *aureofaciens*; ATCC #13985). The product N_2O was analyzed by continuous flow isotope ratio mass spectrometry on a Thermo Delta V Advantage isotope ratio mass spectrometer interfaced with a purpose-built, gas chromatography-based device for N_2O extraction, concentration, and purification (Casciotti et al., 2002; McIlvin & Casciotti, 2011). Nitrite (NO_2^-), which interferes with the NO_3^- isotope analyses, was removed from samples with sulfamic acid (Granger & Sigman, 2009) prior to analysis in the few samples where it was detected.

Individual analyses were referenced to injections from a laboratory standard N_2O tank and calibrated using the NO_3^- reference materials IAEA-N3 (4.7‰ vs. N_2 and 25.6‰ vs. VSMOW; Böhlke et al., 2003; Gonfiantini

et al., 1995) and U.S. Geological Survey-34 (−1.8‰ vs. N_2; −27.9‰ vs. VSMOW; Böhlke et al., 2003), with monitoring of reproducibility by analysis of an internal seawater NO_3^- standard from the deep North Atlantic. NO_3^- standards in individual runs were diluted in nutrient-free seawater to concentrations equivalent to those of samples to account for potential matrix effects on $\delta^{18}O_{NO3}$ measurements (Weigand et al., 2016). In order to ensure measurement accuracy, samples were analyzed in duplicate within runs, for a minimum of three discrete runs, yielding average standard deviations of 0.2‰ for N and 0.3‰ for O, although with a lower precision averaging 0.4‰ for $\delta^{18}O_{NO3}$ at lower NO_3^- concentrations (<10 μM).

Samples for the isotopic analysis of water were collected in plastic screw-capped tubes. The $^{18}O/^{16}O$ ratios of water ($\delta^{18}O_{H2O}$) were analyzed by CO_2 equilibration (Epstein & Mayeda, 1953) on a Micromass AquaPrep system and the CO_2 analyzed on a Micromass IsoPrime universal triple collector isotope ratio mass spectrometer in dual inlet mode at the Université du Québec à Montréal (Light Stable Isotope Geochemistry Laboratory). Data were normalized against two internal reference waters, both calibrated against VSMOW and Vienna Standard Light Antarctic Precipitation. The oxygen isotope measurements are reported on the δ scale in per mille relative to VSMOW. Based on replicate analyses of the samples, the average relative standard deviation of the measurements was better than 0.05‰.

3. Results

3.1. General Hydrography

The observed temperature-salinity relationships reveal features typical of the southeastern Beaufort Sea (e.g., Aagaard et al., 1985; Jones et al., 1991). A fresh surface layer of modified Pacific water extends to 50 m (Figures 2a, 2e, and 3a), overlying slightly saltier Alaska Coastal Water (ACW; $30 < S_P < 32$). ACW is a relatively warm (−1 °C) coastal current that contains a significant river component and enters the Canada Basin from the eastern Chukchi shelf at Barrow Canyon (Figure 1b). The eastward current hugs the Alaskan coast to Barrow Point, joining the anticyclonic Beaufort gyre via the Alaskan Coast (Münchow & Carmack, 1997; Paquette & Bourke, 1974; Pickart et al., 2005; Shimada et al., 2006; Spall et al., 2008). ACW is underlain by saltier ($32 < S_P < 33$) Pacific-origin water modified in the summer over the Chukchi Sea, termed Pacific Summer Water (PSW or *summer Bering Shelf Water*; Coachman et al., 1975; Figures 2a, 2e, and 3a). PSW drains into the upper halocline of the Canada Basin at Harold Canyon and Barrow Canyon (Figure 1b; Linders et al., 2017; Weingartner et al., 1998). A temperature maximum is associated with PSW in the northern Beaufort Gyre but is absent in the southern gyre (Figures 2a, 2e, and 3a; Shimada et al., 2001; Steele et al., 2004; Timmermans et al., 2014). Pacific-origin water with higher salinity ($33 < S_p < 33.5$) and a temperature minimum (−1.5 °C), termed Pacific Winter Water (PWW or *winter Bering Shelf Water*; Coachman et al., 1975), underlies PSW. Its physical properties are akin to those of waters passing through Bering Strait in winter (Coachman & Barnes, 1961), but interaction with shelf sediments is required to explain its chemical properties (Jones & Anderson, 1986; Moore & Smith, 1986; Walsh et al., 1989). As evidenced further below, PWW is associated with a prominent O_2 deficit and elevated nutrient concentrations (Falkner et al., 2005; Jones & Anderson, 1986; Moore et al., 1983; Walsh et al., 1989). More saline (>33.5) and warmer Atlantic-derived waters underlie PWW from 200 to 1,500 m (Coachman & Barnes, 1961; Rudels et al., 1996). These originate from the Norwegian and Greenland Seas, entering the Eurasian basin from the Barents Sea shelf and through Fram Strait (Jones et al., 1998). The lower Atlantic halocline (250 m) centered at a S_P ~ 34.3 (Rudels et al., 1996) derives in part from the Barents Sea branch, whereas core AW below (400 m), which is associated with a temperature maximum of 0.7 °C (S_P ~ 34.8), derives from the West Spitsbergen Current at Fram Strait. Below the temperature maximum, AW is ventilated by deep waters of the Greenland and Norwegian Seas (Bönisch & Schlosser, 1995; Marnela et al., 2016). Underlying AW, Canada Basin Deep Water (CBDW) is also of Atlantic origin but horizontally isolated from the Eurasian basin by the Losomonov Ridge (below 1,700 m) and from the Makarov Basin by the Alpha and Mendeleyev Ridges (below 2,400 m). As such, CBDW is presently not ventilated (Macdonald & Carmack, 1991; Timmermans et al., 2003; Timmermans & Garrett, 2006), with a corresponding ^{14}C isolation age estimated at 450 years below 2,200 m (Schlosser et al., 1997).

3.2. Biogeochemical Tracer Distributions

The depth distribution of [NO_3^-] in the southern gyre was similar among stations. [NO_3^-] was undetectable in surface waters, increasing progressively below 50 m to a maximum of ≥16 μM at 150 m, coincident with the

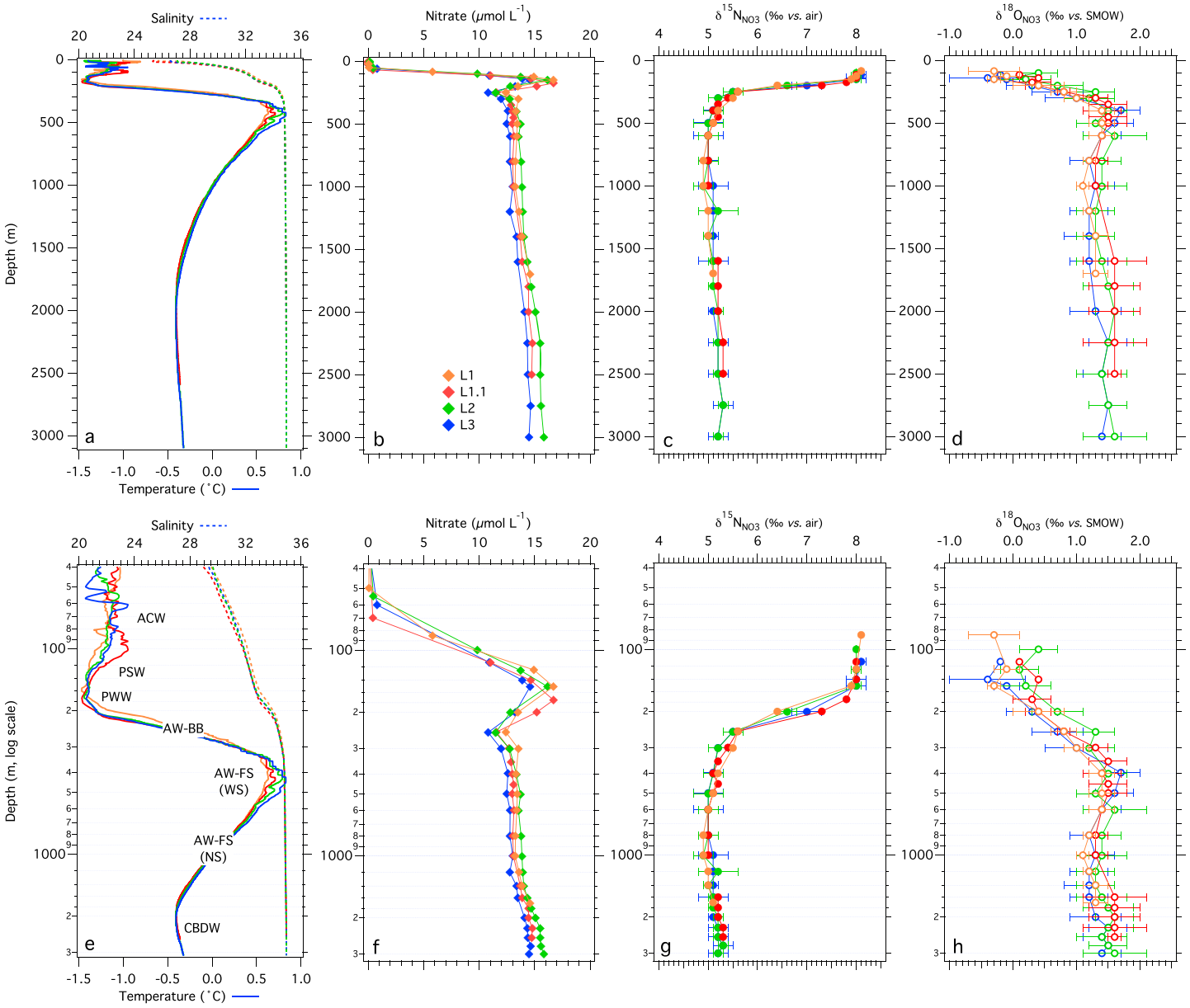

Figure 2. Depth profiles of (a, e) salinity and temperature, (b, f) NO_3^- concentration (c, g) $\delta^{15}N_{NO3}$, and (d, h) $\delta^{18}O_{NO3}$ at hydrographic stations in the southeastern Canada Basin. Depth is presented on a logarithmic scale in (e) and (f), spanning 40–3,100 m. AW-BB indicates Barents Branch Atlantic Water, AW-FS is Fram Strait Atlantic Water, from the West Spitsbergen Current (WS) or from the deep Nordic Seas (NS). CBDW = Canada Basin Deep Water; PSW = Pacific Summer Water; PWW = Pacific Winter Water; SMOW = standard mean ocean water.

temperature minimum of PWW (S_P ~ 33.1; Figures 2b, 2f, and 3b; Table 1). [NO_3^-] decreased to ≤12 μM at 250 m (S_P ~ 34.3) in the Atlantic halocline, increasing slightly to 13 μM at the temperature maximum in core AW at 400 m (S_P ~ 34.8 salinity) and further increasing with depth to a maximum of 16 μM at 3,000 m in CBDW.

Maxima in the concentrations of SRP (1.9 μM; Figure 3c) and silicic acid (40 μM; supporting information Figure S1) were also evident in PWW, coincident with the NO_3^- peak. SRP concentrations decreased to a minimum of 0.8 μM in the Atlantic halocline (S_P ~ 34.3), increasing to 0.9 μM in core AW then to 1.1 μM in CBDW. Silicic acid concentrations decreased to 10 μM at S_P ~ 34.3 in the Atlantic halocline, to a minimum of 7 μM in core AW then increased in CBDW to nearly 15 μM at 3,000 m (Figure S1; Table 1).

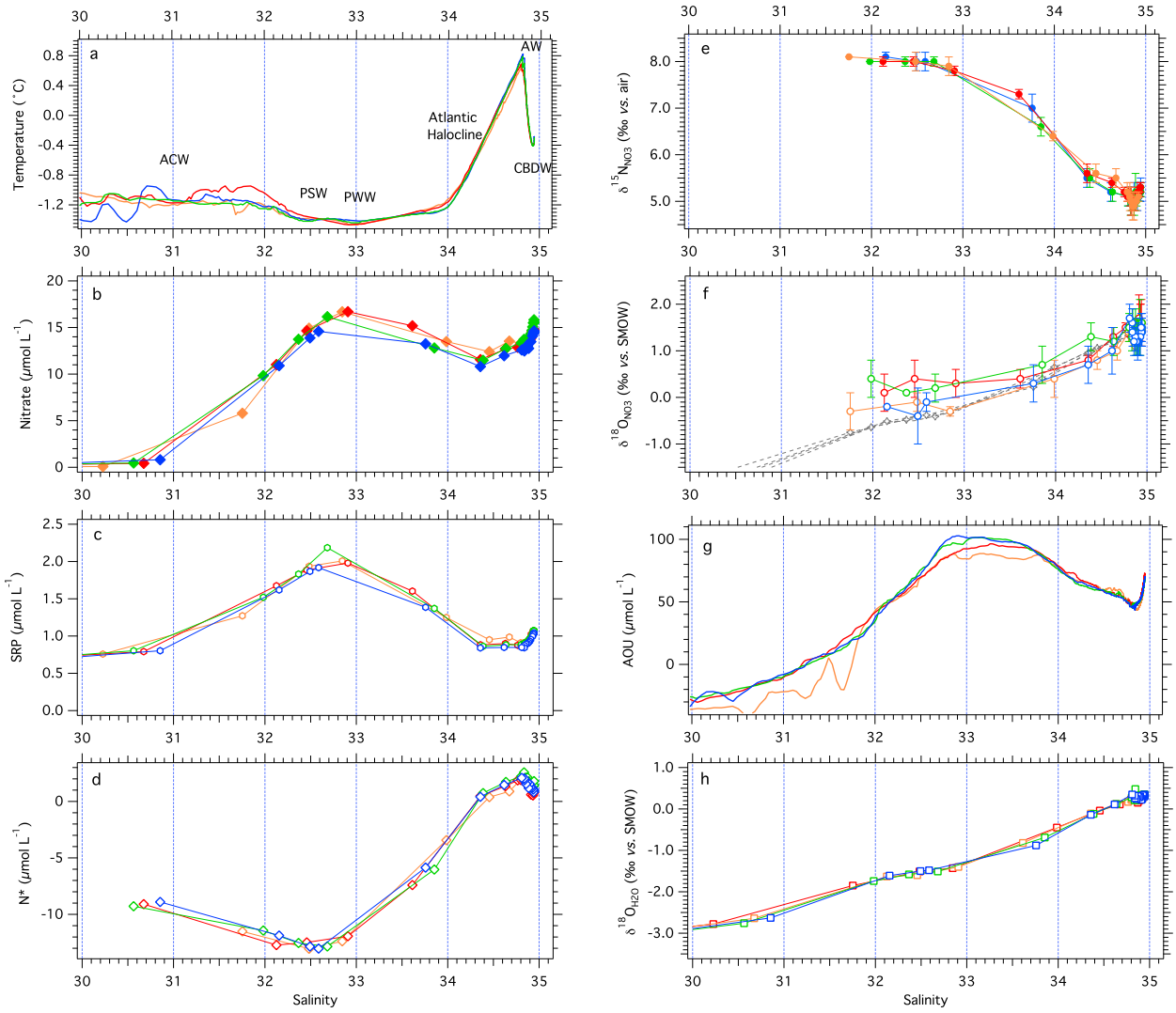

Figure 3. Tracer distributions at hydrographic stations in the southeastern Canada Basin plotted versus salinity: (a) Temperature, (b) NO_3^- concentration, (c) SRP concentration, (d) N*, (e) $\delta^{15}N_{NO3}$, (f) $\delta^{18}O_{NO3}$ in colors and $\delta^{18}O_{NO3}$ expected for nitrification NO_3^- = $\delta^{18}O_{H2O}$ + 1.1‰ in gray, (g) AOU, and (h) $\delta^{18}O_{H2O}$. Surface measurements ($P_s < 30$) are omitted. ACW = Alaska Coastal Water; AOU = apparent oxygen utilization; AW = Atlantic Water; CBDW = Canada Basin Deep Water; PSW = Pacific Summer Water; PWW = Pacific Winter Water; SMOW = Standard Mean Ocean Water; SRP = soluble reactive phosphate.

The $[NO_3^-]$ maximum in PWW was associated with an N* minimum of −13 μM (where N* is defined as $[NO_3^-]$ – 16 * [SRP] + 2.9; Gruber & Sarmiento, 1997), indicating substantial depletion in NO_3^- relative to SRP (Figure 3d; Table 1)—assuming remineralization of organic material with Redfield (1934) stoichiometry.

Table 1
Binned Averages of Biogeochemical Properties of Water Masses (Defined by Salinity and Temperature) at Hydrographic Stations in the Eastern Beaufort Sea

Water mass	Salinity (S_p)	Temp. (°C)	NO_3^- (μM)	SRP (μM)	Si (μM)	N* (μM)	AOU (μM)	$\delta^{18}O_{H2O}$ (‰ vs. SMOW)	$\delta^{18}O_{NO3}$ (‰ vs. SMOW)	$\delta^{15}N_{NO3}$ (‰ vs. air)
PWW	33.1	−1.5	16	1.9	40	−13	95	−1.2	0.0 ± 0.3	8.0 ± 0.1
AW (Barents Branch)	34.3	−0.6	12	0.8	10	0	65	−0.2	0.9 ± 0.3	5.6 ± 0.1
AW (West Spitsbergen)	34.8	0.7	13	0.8	7	3	45	0.3	1.5 ± 0.1	5.2 ± 0.1
AW (deep Nordic Seas)	34.85	−0.4	14	0.9	10	2	55	0.3	1.3 ± 0.1	4.9 ± 0.0
CBDW	34.94	−0.3	16	1.1	15	1	60	0.3	1.5 ± 0.2	5.2 ± 0.1

Note. AOU = apparent oxygen utilization; AW = Atlantic Water; CBDW = Canada Basin Deep Water; PWW = Pacific Winter Water; SMOW = Standard Mean Ocean Water; SRP = soluble reactive phosphate.

N* increased in the Atlantic halocline to positive values (+3 μM) at the temperature maximum in core AW and decreased slightly to +1 μM in CBDW.

Depth profiles of the N and O isotope ratios of NO_3^- were indistinguishable among stations but showed distinctive values within the constituent water masses (Figures 2 and 3e; Table 1). A conspicuous $\delta^{15}N_{NO3}$ maximum of 8‰ was associated with the [NO_3^-] maximum and N* minimum in PWW. $\delta^{15}N_{NO3}$ was similar in waters above, PSW and ACW, despite a progressive decrease in [NO_3^-] toward the surface. Below PWW, $\delta^{15}N_{NO3}$ decreased through the Atlantic halocline to 5.6‰ at S_P ~ 34.3 then 5.2‰ at the temperature maximum of AW (S_P ~ 34.8 at 400 m), decreasing to a minimum of 4.9‰ at S_P ~ 34.85 between 700 and 1,200 m then increasing again to 5.3‰ in CBDW.

In contrast to $\delta^{15}N_{NO3}$, $\delta^{18}O_{NO3}$ values were the lowest in PWW (S_p ~ 33.1), approximately 0‰ at 150 m (Figures 2 and 3f; Table 1). Like $\delta^{15}N_{NO3}$, $\delta^{18}O_{NO3}$ was similar in PSW and ACW to that in PWW despite the upward decrease in [NO_3^-] into PSW and ACW. In AW below, $\delta^{18}O_{NO3}$ values increased progressively to a maximum of 1.5‰ in core AW at the temperature maximum (400 m) then decreased to a minimum of 1.3‰ between 700 and 1,200 m (Figure 2h). Values then increased in CBDW to +1.5‰.

Apparent oxygen utilization (AOU; Broecker & Peng, 1983), the difference between saturation (Weiss, 1970) and measured O_2 concentrations, was negative (above saturation) in ACW, increasing to a salient maximum of 80–100 μM in PWW (Figure 3g; Table 1). AOU decreased to ≤50 μM at the temperature maximum in core AW then increased again to ~60 μM in CBDW.

Depth profiles of $\delta^{18}O_{H2O}$ at all hydrographic stations revealed low values of −3.5‰ in the surface polar mixed layer, increasing to −3‰ in ACW below and to −1.5‰ in PWW (Figure 3h; Table 1). Values increased through the Atlantic halocline to 0.3‰ in core AW and in CBDW below.

4. Discussion

The N and O isotope ratios of NO_3^- reveal distinctive features associated with water masses of the southern Beaufort Sea. Tracer distributions in the Pacific halocline inform on the physical and biogeochemical processes that give rise to nutrient maxima in this depth interval. In AW, NO_3^- isotope ratios differ between the temperature maximum layer and the deeper AW, providing insights into the origins of NO_3^- therein. In CBDW, the NO_3^- isotope ratios and complementary tracers provide evidence of modifications from remineralization of organic matter and may also record a signal from benthic denitrification. We first discuss features of the Pacific halocline, followed by those of AW and CBDW.

4.1. Insights on the Ventilation of the Pacific Halocline

The $\delta^{15}N_{NO3}$ maximum and corresponding $\delta^{18}O_{NO3}$ minimum associated with the nutrient peaks in the Pacific halocline (S_p ~ 33.1) are the most salient features of the NO_3^- isotope depth profiles. These features pervade PWW in the western Arctic Basin, having also been observed off the slope of the eastern Chukchi shelf and off of the East Siberian shelf (Brown et al., 2015; Fripiat et al., 2018). At our stations, the $\delta^{15}N_{NO3}$ increases to 8‰ in PWW, compared to 5.6‰ in the Atlantic halocline below, which could be interpreted as signaling NO_3^- consumption at the subsurface, from assimilation or water-column denitrification, processes that discriminate equivalently against the heavier N (and O) isotopologues of NO_3^- (Granger et al., 2004, 2008). However, $\delta^{18}O_{NO3}$ values decrease concurrently from ~1‰ in the Atlantic halocline to ~0‰ in PWW, while NO_3^- concentrations increase to a maximum in PWW—thus discounting subsurface consumption to explain the elevated $\delta^{15}N_{NO3}$ of PWW.

From PWW (S_p ~ 33.1 at 150 m) toward the surface, $\delta^{15}N_{NO3}$ and $\delta^{18}O_{NO3}$ remain relatively invariant at 8‰ and 0‰, respectively, whereas [NO_3^-] decreases to below detection at 50 m, further arguing that NO_3^- assimilation does not drive the elevated $\delta^{15}N_{NO3}$ in PWW (Figure 2). The constant $\delta^{15}N_{NO3}$ and $\delta^{18}O_{NO3}$ values between 150 and 50 m, in light of decreasing [NO_3^-], are best explained by mixing of NO_3^--deplete PSW and ACW with NO_3^--rich PWW, such that the $\delta^{15}N_{NO3}$ of PWW is observed throughout the upper water column. Diapycnal mixing of these water masses is borne out of an optimum multiparameter analysis of the source water contributions (Lansard et al., 2012).

To uncover the processes that lead to the elevated concentration and distinct isotopic composition of NO_3^- in PWW, we first examine the origin of the associated $\delta^{18}O_{NO3}$ minimum. The $\delta^{18}O_{NO3}$ decrease from the lower Atlantic halocline into PWW approximately mirrors a coincident decrease in $\delta^{18}O_{H2O}$ (Figure 3). This association reveals that NO_3^- is largely remineralized: Nitrification—the biological oxidation of ammonium to NO_3^-—produces NO_3^- with an empirical $\delta^{18}O_{NO3}$ value of approximately +1.1 ‰ above that of ambient water (Buchwald et al., 2012; Casciotti et al., 2008; Sigman et al., 2009). Based on this empirical metric (i.e., $\delta^{18}O_{NO3,nitrified} = \delta^{18}O_{H2O} + 1.1‰$), we approximate that NO_3^- in core PWW is largely newly nitrified: Given a $\delta^{18}O_{H2O,150m} = -1.2‰$, nitrified NO_3^- is expectedly on the order −0.1‰, indistinguishable from the $\delta^{18}O_{NO3}$ observed in PWW. This estimate relies on the assumption that the corresponding $\delta^{18}O_{H2O}$ reflects that at the time of nitrification—which may be inaccurate due to diapycnal mixing with the Atlantic halocline below and the PWW above (Melling et al., 1984; Wallace et al., 1987; Woodgate et al., 2005). Nevertheless, the $\delta^{18}O_{NO3}$ associated with PWW in the Beaufort Gyre suggests that NO_3^- is predominantly remineralized (Granger et al., 2011). This inference echoes parallel interpretations inferred from $\delta^{18}O_{NO3}$ measurements in PWW off the eastern Chukchi slope (Brown et al., 2015) and the East Siberian shelf (Fripiat et al., 2018).

The $\delta^{18}O_{NO3}$ of PWW in the Canada Basin is notably lower than that of the Pacific end-member at the surface waters of the Bering Sea of ~2.5‰ (Granger et al., 2011). This difference implies that the regenerated $\delta^{18}O_{NO3}$ signal in PWW was likely acquired in transit on the productive continental shelves, the Bering Sea shelf and/or the Chukchi shelf (Brown et al., 2015; Jones & Anderson, 1986). Particle export in the western basin itself has been discounted as a significant source of nutrients to the halocline nutrient maxima, given the low surface productivity of the basin (Wallace et al., 1987; Walsh et al., 1989). In this respect, the $\delta^{18}O_{NO3}$ values between 50 and 150 m appear relatively invariant, within uncertainty (± 0.5‰), whereas $\delta^{18}O_{H2O}$ values increase by ~0.8‰ in this depth interval (Figure 3). These differing trends suggest that nitrification within the basin is not responsible for the bulk of the NO_3^- at these depths, as the $\delta^{18}O$ of newly remineralized NO_3^- in the subsurface would be expected to mirror $\delta^{18}O_{H2O}$. NO_3^- isotope ratios in PWW and above thus appear to capture a signal imparted upstream in the circulation, on the shelf.

The coincident AOU signal of PWW further evidences a poorly ventilated water mass, suggesting that NO_3^- was regenerated in isolation from the sea surface. Such a dynamic is expected on the Chukchi shelf in summer and fall, when PWW on the shelf is restricted to a deeper layer in proximity of the sediments—referred to as *remnant* PWW (*r*PWW; Gong & Pickart, 2015). *r*PWW in summertime is overlain by fresher and warmer water from sea ice melt, thus isolated from the surface by a density barrier (Gong & Pickart, 2015; Woodgate et al., 2005). The shelf is highly productive in spring through summer, at which time nutrients are drawn down in the surface layer and regenerated in the subsurface, with a commensurate consumption of oxygen (Figure 4; Lowry et al., 2015; Nishino et al., 2016). *r*PWW thus accumulates nutrients and AOU in summer (Figure 4). Conversely, in winter, salinization from sea ice formation results in an isohaline water column with the salinity and temperature characteristics of PWW (Figure 4; Woodgate et al., 2005). Although sea ice cover substantially curtails gas exchange with the atmosphere (Butterworth & Miller, 2016), a few published data indicate that O_2 concentrations on the Chukchi shelf in winter are at ~90% of saturation (Nishino et al., 2016), suggesting sufficient exchange to counter any substantial O_2 consumption by respiration. The O_2 concentrations in wintertime shelf PWW are thus not sufficiently low to explain its depletion in PWW downstream. The association of the nutrient maxima with a substantial AOU otherwise suggests that shelf *r*PWW is that which ventilates the basin, predominantly in summer (Figure 4).

To gauge whether PWW on the shelf ventilates the basin largely when it is isolated from the sea surface (as *r*PWW), we examine the adherence of AOU-to-nutrient ratios of PWW in the Canada Basin to the remineralization stoichiometry of organic material. Based on the stoichiometry of Anderson and Sarmiento (1994; −170 O_2: 1 P), the AOU maximum of 90 μM at our stations accounts for the regeneration of 32% of ambient SRP. The regeneration of SRP associated with benthic denitrification cannot explain the difference, accounting for only 5% of the ambient SRP (Redfield et al., 1963). Closer to the Chukchi shelf, where biogeochemical signals in PWW are expectedly less diluted by diapycnal mixing, O_2 concentrations in PWW can be as low as 130 μM (Swift et al., 1997), compared to 270 μM at our stations. The corresponding AOU of 230 μM accounts for 75% of the ambient SRP. Thus, AOU does not account for the whole of nutrient concentrations of basin PWW. This apparent discrepancy could arise from different scenarios. First, the computations above do not

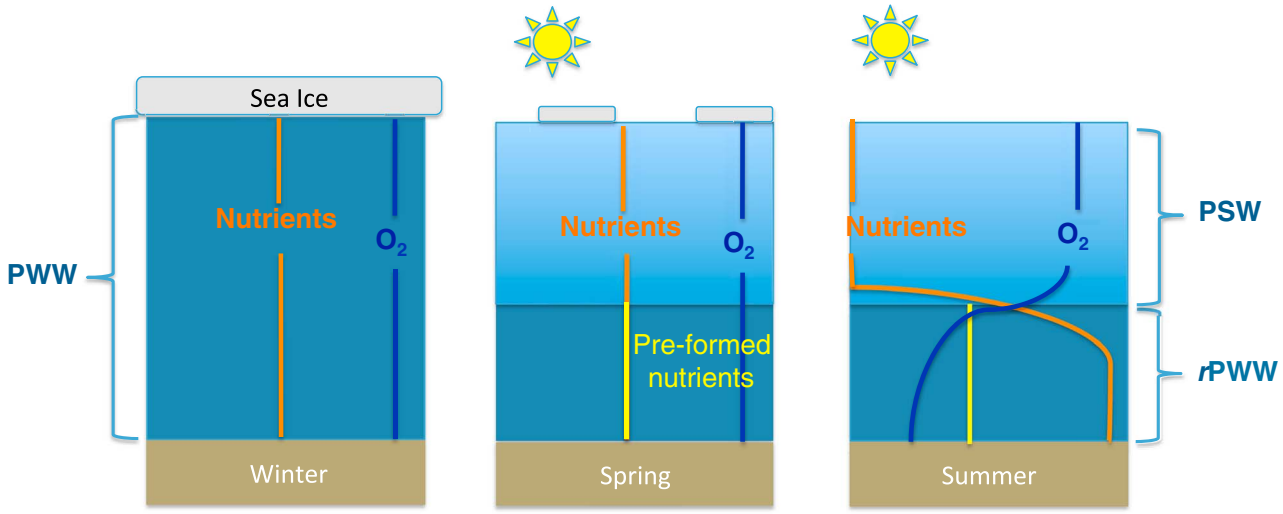

Figure 4. Schematic of seasonal nutrient and oxygen dynamics on the Chukchi shelf. (a) Nutrients and oxygen concentrations on the ice-covered shelf are homogenous in isohaline PWW. Oxygen concentrations approach saturation. (b) Ice melt and solar insolation freshen and warm the surface layer, isolating *r*PWW from PSW at the surface prior to significant nutrient consumption by phytoplankton. (c) Nutrients are consumed by primary producers at the surface and remineralized at depth following export of organic material to the benthos. Remineralized nutrients are added to the preformed pool. Oxygen is consumed in proportion to the remineralized nutrients. PSW = Pacific Summer Water; PWW = Pacific Winter Water; *r*PWW = *remnant* Pacific Winter Water.

include preformed nutrients (Redfield, 1958), which are not associated with a commensurate AOU signal. In winter, bulk nutrients in shelf PWW would contribute to preformed nutrients once the water is isolated from the surface (Figure 4). In spring and summer, with the onset of stratification, a portion of the unused nutrients in the winter mixed layer becomes preformed nutrients in now-isolated *r*PWW. Remineralized nutrients are then progressively added to preformed nutrients in *r*PWW from the decay of exported organic material during the growing season, with a commensurate increase in AOU. Second, diapycnal mixing during upwelling at the slope (Melling et al., 1984; Münchow & Carmack, 1997; Pickart et al., 2005; Woodgate et al., 2005) likely erodes the original AOU-to-nutrient ratios incurred on the shelf due to mixing with Atlantic halocline below and PSW and ACW above (see Lansard et al., 2012). Finally, the stoichiometry of remineralization on the Chukchi shelf may differ from that of L. A. Anderson and Sarmiento (1994), a hypothesis for which there is evidence (Mills et al., 2015). In all, while the formation of the nutrient and AOU maxima in the basin is better explained by ventilation with shelf *r*PWW in summer, some contribution of shelf PWW with low AOU (in winter) cannot be discounted from the biogeochemical tracers examined here.

The insights above illuminate some perplexing aspects of the development of the nutrient maxima in PWW. By definition, PWW is that having temperature and salinity characteristics closely resembling those of waters passing through Bering Strait in *winter* (Coachman & Barnes, 1961). The nutrient maxima in PWW were thus originally construed as a signature of Bering Sea water at Bering Strait in winter, with possible modifications by shelf processes (Aagaard et al., 1981; Coachman et al., 1975; Kinney et al., 1970). Subsequently, Moore et al. (1983) suggested that nutrients in PWW reflect source waters from the Bering Sea, noting that primary production on the Bering and Arctic shelves would result in the accumulation of nutrients in waters overlying the sediments, propagating as overflows of nutrient-rich water into the halocline. Subsequently, given reasonable agreement of PWW tracers in the basin with Redfield nutrient stoichiometry (Redfield et al., 1963), Jones and Anderson (1986) reasoned that O_2 undersaturation is unlikely for water passing over the 45-m-deep sill at Bering Strait, where they would likely oxygenate upon exposure to the atmosphere. The authors thus posited that PWW reflects the products of summer remineralization specifically on adjacent Arctic shelf sediments, further speculating that remineralized tracers are entrained off-shelf by brines sinking to the bottom during ice formation, in early winter. However, Cooper et al. (1997) later argued that, because inorganic nutrient concentrations in summer at Bering Strait and on the Chukchi shelf are less than those of the nutrient maxima of the western basin, the biogeochemical properties of basin PWW require that it be maintained by winter outflow from the shelf, largely unmodified by biota. Under the premise that PWW ventilates the

Arctic halocline specifically in winter (e.g., Cooper et al., 1997; Melling & Moore, 1995), contrary to the argument put forth here that PWW ventilation from the shelf occurs in summer, Brown et al. (2016) then proposed a mechanism by which PWW in the basin could retain dissolved inorganic carbon (DIC) concentrations in excess of equilibrium as well as a low carbon isotope composition ($\delta^{13}C$) of DIC—derived from the remineralization of organic material on the shelf—in light of an isohaline winter water column, arguing that sea ice cover only permits limited equilibration of remineralized DIC (and AOU) with the atmosphere. In summary, posited mechanisms of Pacific halocline ventilation differ, although most researchers at this junction concur that biogeochemical tracers in PWW reflect a remineralization signal from the Chuckchi shelf. The means by which PWW retains elevated AOU and remineralized DIC tracers in light of potential wintertime ventilation remain unclear.

Contrary to the assumption in some biogeochemical literature that PWW ventilates the basin in winter, physical observations of shelf flows and of basin ventilation at submarine canyons bordering the Arctic Basin provide some resolution regarding the formation of the nutrient maxima, revealing that PWW ventilates the basin primarily in summer (Münchow & Carmack, 1997; Pickart et al., 2005; Weingartner et al., 1998, 2017; Woodgate et al., 2005), as surmised here. In late fall through winter, the winds out of the northeast intensify (Furey, 1996; as cited by Pickart et al., 2005), substantially retarding or reversing the northward flow at Bering Strait, with the mean transport in winter not differing significantly from zero, whilst the autumn maximum lies at ~1.5 Sv (Roach et al., 1995; Woodgate et al., 2005). Weaker water flow is consequently observed over the Chukchi shelf and in Herald Valley in winter (Woodgate et al., 2005). The off-shelf flow at Barrow Canyon is also low, or absent, during winter months (Münchow & Carmack, 1997; Pickart et al., 2005; Weingartner et al., 1998, 2017; Woodgate et al., 2005). Northeasterly winds subside in springtime, at which point PWW flows through Barrow Canyon as a subsurface current that lasts for several months (Mountain et al., 1976), persisting beneath the buoyant Alaskan Coastal Current during the late summer (Münchow & Carmack, 1997; Paquette & Bourke, 1974; Pickart et al., 2005). Thus, while PWW on the shelf is technically formed in winter, the remnant of PWW at the shelf bottom is that which advects off shelf largely in summer, presumably retaining AOU accrued from the remineralization of organic material during the growing season.

The low $\delta^{18}O_{NO3}$ observed in PWW is consistent with the above mechanism, suggesting that NO_3^- therein is predominantly regenerated. From the perspective of the AOU-based definition of preformed and regenerated nutrients, however, ~25% of nutrients in PWW are preformed. The $\delta^{18}O_{NO3}$ signal then implies that even preformed nutrients derive from an environment with no coincident NO_3^- assimilation, where the last biological transformation to influence preformed NO_3^- was nitrification. In contrast, preformed NO_3^- originating from the Southern Ocean is isotopically enriched, bearing the imprints of its partial assimilation at the Antarctic surface prior to subduction (Rafter et al., 2013). Similarly, NO_3^- imported at the shallow (≤35 m) Bering Strait in summer (in PSW) has elevated $\delta^{18}O_{NO3}$ values of ≥6‰ (Brown et al., 2015)—due to partial NO_3^- assimilation—while NO_3^- isotope ratios at Bering Strait in winter have not been measured. We interpret these observations as follows: During the growing season, NO_3^- at the Chukchi shelf surface is completely assimilated, removing any potential for the accumulation of residual of high $\delta^{18}O_{NO3}$. Organic matter is remineralized at the subsurface, producing characteristically low $\delta^{18}O_{NO3}$ and increasing AOU. During ice formation, the water column becomes isohaline, homogenizing subsurface NO_3^- throughout. NO_3^- assimilation, however, is curtailed due to the absence of light, such that $\delta^{18}O_{NO3}$ remains at the low values of nitrification NO_3^-, whereas AOU is lost to gas exchange. Upon restratification during ice melt, subsurface waters have low AOU and low $\delta^{18}O_{NO3}$ values of a NO_3^- pool that now qualifies as *preformed*. This scenario is partly validated by observations on the adjacent Bering Sea shelf, where NO_3^- in the ice-covered water column is produced by nitrification during the winter months (Whitledge et al., 1986), and where the $\delta^{18}O_{NO3}$ values in early spring prior to ice retreat are low, indicating that the NO_3^- pool was produced in the absence of assimilation (Granger et al., 2013). Moreover, $\delta^{18}O_{NO3}$ values observed in *r*PWW on the northern Chukchi shelf in summer are coherently low (Brown et al., 2015), as observed downstream in basin PWW. In short, preformed NO_3^- in basin PWW is not isotopically distinct from remineralized NO_3^- due to complete NO_3^- assimilation at the shelf surface in summer and no assimilation during periods of ventilation in winter.

The regenerated nature of NO_3^- in PWW, in-and-of-itself, does not explain its relatively elevated $\delta^{15}N$ of 8‰. The end-member $\delta^{15}N_{NO3}$ in surface Bering Sea waters is ~6.5‰ in late summer (Granger et al., 2011), thus lower than that measured in PWW, such that $\delta^{15}N_{NO3}$ is evidently modified in transit on the Bering and

Chukchi shelves. Indeed, Granger et al. (2011) and Brown et al. (2015) reported that the $\delta^{15}N$ of reactive N on the Bering and Chukchi shelves increases progressively in proportion to N loss recorded by N* in the water column, ascribing the increase to coupled nitrification-denitrification in shelf sediments: Nitrogen isotopic discrimination of reactive N occurs during nitrification of ammonium to NO_3^- in sediments, resulting in ^{15}N enrichment of benthic ammonium and the production of ^{15}N-deplete NO_3^-. The ^{15}N-deplete nitrate is denitrified to N_2 in underlying sediments, whereas the ^{15}N-enriched ammonium is released to the water column (Granger et al., 2011; Morales et al., 2014). Complete nitrification of water-column ammonium then yields ^{15}N-enriched, ^{18}O-deplete NO_3^-, consistent with the signal observed downstream in PWW. The imprint of coupled nitrification-denitrification then propagates to the Pacific halocline of the Arctic Ocean, where the $\delta^{15}N_{NO3}$ maximum coincides with the N* minimum of PWW (Granger et al., 2011). Close examination reveals that the N* minimum actually lies slightly *above* the nutrient and $\delta^{15}N_{NO3}$ maxima, which is explained by diapycnal mixing of SRP-rich Pacific water with SRP-poor AW below. Thus, the $\delta^{15}N_{NO3}$ in PWW bears the imprint of benthic N loss on the Bering and Chukchi shelves (Brown et al., 2015; Granger et al., 2011).

One conundrum remains regarding the mechanism for PWW formation proposed here, namely, that nutrient concentrations on the Chukchi shelf are reportedly insufficient in summer to explain the more elevated concentrations in the basin (Cooper et al., 1997). Nonetheless, nutrient concentrations in *r*PWW on the Chukchi shelf post concentrations comparable to those in the basin, with silicic acid on the order 40 to 60 μM (Lowry et al., 2015; Pisareva et al., 2015). Likewise, observations on the East Siberian shelf, whose waters contribute to the outflow at Harold Canyon (Linders et al., 2017), also reveal considerably elevated nutrient concentrations, with silicic acid at the subsurface reaching 60 μM (Anderson et al., 2013)— ample to explain corresponding maxima in the basin. Thus, nutrients in combined summer *r*PWW outflows at the Chukchi shelf canyons appear sufficient to explain the nutrient maxima of PWW downstream in the basin.

4.2. Sources of NO_3^- in AW and CBDW

Underlying the Upper Pacific halocline of the Canada Basin, the lower Atlantic halocline derives from the Norwegian Sea and ultimately from the North Atlantic. The lower halocline in the southern Canada Basin specifically originates from the upper part of the Barents Sea Branch that enters the Arctic Ocean through the Santa Anna Trough, distinct from the underlying Fram Strait Branch of AW (Rudels et al., 2004). Formation of the Barents Sea Branch halocline remains debated but involves vertical mixing of cold, less saline Eurasian shelf waters with warm AW at the continental slope, resulting in a salinity-stratified thermocline (Dmitrenko et al., 2012; Rudels et al., 2004). The Barents Branch halocline end-member at 250 m (S_P ~ 34.3) is distinguished by low nutrient concentrations and a characteristically low value for the semiconservative tracer NO ($NO = [O_2] + 9\,[NO_3^-]$) (Broecker, 1974); Figure S1b) posited to reflect lower $[NO_3^-]$ in Barents shelf waters (Jones & Anderson, 1986; Jones et al., 1998). Given the relatively low $[NO_3^-]$ in the Barents Branch end-member, the $\delta^{15}N_{NO3}$ of 5.6‰ and $\delta^{18}O$ of 0.9‰ of AW may largely derive from mixing-associated input of NO_3^- from overlying PWW (Figures 2f and 2g).

Below the Barents Branch, nitrogen tracers at the temperature maximum of core AW ($\delta^{15}N_{NO3}$ of 5.2‰, $\delta^{18}O_{NO3}$ of 1.5‰, and positive N*; Figures 2 and 3) coincide roughly with those of North Atlantic Deep Water (Gruber & Sarmiento, 1997; Marconi et al., 2015), albeit, with slightly higher $\delta^{15}N_{NO3}$ (compared to 4.9‰ in North Atlantic Deep Water; Marconi et al., 2015). The Nordic seas that communicate with the Arctic Eurasian Basin are fed from the subpolar Atlantic across the Greenland Scotland Ridge, where North Atlantic Deep Water forms. Specifically, the temperature maximum in the Arctic Basin derives from the warm West Spitsbergen current that branches off the Norwegian Atlantic current—composed primarily of the North Atlantic Drift with some contribution from the North Sea.

AW below the temperature maximum originates from deeper inflows of the Greenland and Norwegian Seas (see Bönisch & Schlosser, 1995). The distinct origins of these deeper AWs are manifest in the NO_3^- isotopes, as both $\delta^{15}N_{NO3}$ and $\delta^{18}O_{NO3}$ values *decrease* below the temperature maximum to respective values of 4.9‰ and 1.3‰ between 700 and 1,500 m (Figure 2). The lower $\delta^{18}O_{NO3}$ suggests a dominant proportion of remineralized NO_3^- from the deep Nordic Seas, given a coincident $\delta^{18}O$ of water of ~0.3‰ (where $\delta^{18}O_{NO3,nitrified} = 0.3‰\,(H_2O) + 1.1‰ = 1.4‰$). The corresponding $\delta^{15}N_{NO3}$ would then derive from the remineralization of organic material produced by assimilation of NO_3^- with a $\delta^{15}N_{NO3}$ of ~4.9‰. However, AOU at corresponding depths is 50 μM, which only accounts for 40% of the ambient NO_3^- (Anderson & Sarmiento,

1994). This discrepancy suggests that the $\delta^{18}O_{NO3}$ of preformed NO_3^- in the Nordic Seas is relatively low, thus also newly nitrified. This feature may arise because deep water convection in the Nordic Seas is restricted to the Greenland Sea gyre during dark winter months (Rudels, 1995; Watson et al., 1999), at which time recently regenerated NO_3^- would not be partially consumed (thus not ^{18}O-enriched) while gas exchange would drive a decrease in AOU. Direct measurements of NO_3^- isotope ratios in these basins would allow for an evaluation of this interpretation.

In CBDW, NO_3^- N and O isotope ratios increase concurrently, as do nutrient concentrations and AOU, while N* decreases relative to the overlying AW (Figures 2 and 3). Presuming that CBDW derives from AW above, the difference in most tracers can be ascribed to mineralization signals accrued in CBDW. CBDW is hypothesized to derive from a relic water mass that ventilated the basin 450 years ago, possibly during the Little Ice Age (Schlosser et al., 1997). In this context, the increase in AOU and decrease in N* are consistent with water column and sediment remineralization, as is the increase in nutrient concentrations relative to AW. The higher $\delta^{15}N_{NO3}$ could then reflect a contribution of regenerated organic material from surface primary production fueled by Pacific-derived NO_3^- and its elevated $\delta^{15}N_{NO3}$.

The corresponding increase in $\delta^{18}O_{NO3}$ in CBDW relative to the AW end-member, however, appears inconsistent with this interpretation, as $\delta^{18}O_{NO3}$ should decrease in response to an accumulation of regenerated NO_3^-. The $\delta^{18}O_{NO3}$ and $\delta^{15}N_{NO3}$ increase could otherwise derive from communication of water column NO_3^- with isotopically enriched NO_3^- in denitrifying sediments. Generally, however, N and O isotopic enrichments of NO_3^- at the sediment depth of denitrification are not communicated to the water column reservoir given rapid consumption relative to diffusion (Brandes & Devol, 1997; Lehmann et al., 2004, 2005, 2007). This tenet may take exception in the deep Canada Basin where denitrification rates are exceedingly low: Based on the N* difference between CBDW and AW, integrated from 2,200 m to the bottom, and assuming a ventilation age of 450 years (Schlosser et al., 1997), we estimate a sedimentary denitrification rate on the order of 14 $\mu mol{\cdot}N{\cdot}m^{-2}{\cdot}day^{-1}$ for CBDW—approximately 15-fold slower than that of 230 $\mu mol{\cdot}N{\cdot}m^{-2}{\cdot}day^{-1}$ similarly estimated for the N deficit in the Deep Bering Sea Basin where benthic denitrification imparts a negligible isotope effect of 0–1‰ on water column NO_3^- (Lehmann et al., 2005). Thus, NO_3^- N and O isotope ratios in CBDW may bear a slight imprint of direct benthic denitrification.

The mechanisms invoked above to explain NO_3^- isotope ratios in CBDW have antagonistic effects, as remineralization of organic matter should lower $\delta^{18}O_{NO3}$ to near water values and raise $\delta^{15}N_{NO3}$ in proportion to the $\delta^{15}N$ of sinking material, whereas denitrification would potentially increase both $\delta^{18}O_{NO3}$ and $\delta^{15}N_{NO3}$ equivalently. The simultaneous remineralization and denitrification of NO_3^- in CBDW should then give way to a $\delta^{15}N_{NO3}$ increase with depth that exceeds the corresponding $\delta^{18}O_{NO3}$ increase. This scenario appears consistent with our measurements, as a regression of pooled $\delta^{18}O_{NO3}$ measurements below 2,000 m on corresponding $\delta^{15}N_{NO3}$ yields a slope of ~0.9 (data not shown). Plotted as a function of the logarithm of remaining NO_3^- (derived from N*) as a closed-system Rayleigh model (Mariotti et al., 1981), the $\delta^{15}N_{NO3}$ change corresponds to an approximate N isotope effect for benthic denitrification of 1.5‰. Thus, NO_3^- isotope ratios in CBDW bear the imprint of NO_3^- added by remineralization and of NO_3^- isotopic discrimination by benthic denitrification.

4.3. Summary and Implications

The results presented here highlight the importance of shelf processes in modulating the nutrient content of the Pacific halocline, which hosts the subsurface nutrient reservoir. Lengthening of the growing season in the Arctic could, paradoxically, result in a reduced NO_3^- reservoir in the Pacific halocline—assuming no changes in halocline ventilation—as increased shelf productivity (Arrigo & Van Dijken, 2011) may translate to greater benthic mineralization and N loss to benthic denitrification. Superposed on a prediction of enhanced stratification in the Canada Basin due to increased freshwater delivery and from accelerating gyre circulation (McLaughlin & Carmack, 2010; Toole et al., 2010), a reduced subsurface NO_3^- reservoir may give way to an increasingly oligotrophic, ice-free western Arctic Basin. Moreover, there could be increased export of excess P relative to N from the Arctic to the North Atlantic, contributing to N_2 fixation (Yamamoto-Kawai et al., 2006).

NO_3^- isotope ratios also reveal distinctions with respect to the provenance of NO_3^- in the deeper water masses of the Canada Basin. In particular, the $\delta^{18}O_{NO3}$ of preformed NO_3^- in deeper AW has a remineralized

signature, raising questions regarding nutrient cycling in relation to deep winter convection in the Nordic Seas. In CBDW, biogeochemical tracers suggest accrual of regeneration products relative to AW above, notwithstanding a slight increase in $\delta^{18}O_{NO3}$, which may derive from benthic denitrification. Continued survey of hydrographic and biogeochemical tracers in the basin, particularly in the context of the international GEOTRACES effort, will provide additional constraints to unravel the biogeochemistry of the Arctic Ocean and anticipate its response to warming.

Acknowledgments
We are grateful to Roger François and Maureen Soon for collecting the nitrate isotope samples. Thanks must also go to the CTD data acquisition group in ArcticNet for critical hydrographic measurements and for calibration of the various probes. We also thank all scientists, officers, and crew members of the CCGS Amundsen who participated in the ArcticNet 0903 expedition. Sample collection was supported by the Government of Canada program for the International Polar Year. Sample analysis and data interpretation were enabled by funding from the U.S. National Science Foundation (OCE-1535002 to J. G.; OCE-0960802 to D. M. S.). Nitrate isotope data are posted at the GEOTRACES Data Assembly Centre (GDAC; geotraces.dac@bodc.ac.uk).

References

Aagaard, K., Coachman, L. K., & Carmack, E. (1981). On the halocline of the Arctic Ocean. *Deep-Sea Research*, *28A*, 529–545.
Aagaard, K., Swift, J. H., & Carmack, E. C. (1985). Thermohaline circulation in the Arctic Mediterranean Seas. *Journal of Geophysical Research*, *90*(C3), 4833–4846. https://doi.org/10.1029/JC090iC03p04833
Anderson, L. A., & Sarmiento, J. L. (1994). Redfield ratios of remineralization determined by nutrient data analysis. *Global Biogeochemical Cycles*, *8*(1), 65–80. https://doi.org/10.1029/93GB03318
Anderson, L. G., Andersson, P. S., Björk, G., Jones, E. P., Jutterström, S., & Wåhlström, I. (2013). Source and formation of the upper halocline of the Arctic Ocean. *Journal of Geophysical Research: Oceans*, *118*, 410–421. https://doi.org/10.1029/2012JC008291
Arrigo, K. R., van Dijken, G., & Pabi, S. (2008). Impact of a shrinking Arctic ice cover on marine primary production. *Geophysical Research Letters*, *35*, L19603. https://doi.org/10.1029/2008GL035028
Arrigo, K. R., & Van Dijken, G. L. (2011). Secular trends in Arctic Ocean net primary production. *Journal of Geophysical Research*, *116*, C09011. https://doi.org/10.1029/2011JC007151
Barber, D. G., Galley, R., Asplin, M. G., De Abreu, R., Warner, K. A., Pucko, M., et al. (2009). Perennial pack ice in the southern Beaufort Sea was not as it appeared in the summer of 2009. *Geophysical Research Letters*, *36*, L24501. https://doi.org/10.1029/2009GL041434
Berner, J., Symon, C., Arris, L., Heal, O. W., Assessment., A. C. I., (U.S.), N. S. F, et al. (2005). *Arctic climate impact assessment*. New York, N.Y: Cambridge University Press.
Böhlke, J. K., Mroczkowski, S. J., & Coplen, T. B. (2003). Oxygen isotopes in nitrate: New reference materials for ^{18}O:^{17}O:^{16}O measurements and observations on nitrate-water equilibration. *Rapid Communications in Mass Spectrometry*, *17*(16), 1835–1846. https://doi.org/10.1002/rcm.1123
Bönisch, G., & Schlosser, P. (1995). Deep water formation and exchange rates in the Greenland/Norwegian Seas and the Eurasian Basin of the Arctic Ocean derived from tracer balances. *Progress in Oceanography*, *35*(1), 29–52. https://doi.org/10.1016/0079-6611(95)00004-Z
Brandes, J. A., & Devol, A. H. (1997). Isotopic fractionation of oxygen and nitrogen in coastal marine sediments. *Geochimica et Cosmochimica Acta*, *61*(9), 1793–1801. https://doi.org/10.1016/S0016-7037(97)00041-0
Broecker, W. S. (1974). "NO", a conservative water-mass tracer. *Earth and Planetary Science Letters*, *23*(1), 100–107. https://doi.org/10.1016/0012-821X(74)90036-3
Broecker, W. S., & Peng, T. H. (1983). *Tracers in the sea*. Palisades, NY: Lamont-Doherty Geological Observatory.
Brown, K. A., McLaughlin, F., Tortell, P. D., Yamamoto-Kawai, M., & Francois, R. (2016). Sources of dissolved inorganic carbon to the Canada Basin halocline: A multitracer study. *Journal of Geophysical Research: Oceans*, *121*, 2981–2936. https://doi.org/10.1002/2015JC011535
Brown, Z. W., Casciotti, K. L., Pickart, R. S., Swift, J. H., & Arrigo, K. R. (2015). Aspects of the marine nitrogen cycle of the Chukchi Sea Shelf and Canada Basin. *Deep-Sea Research Part II: Topical Studies in Oceanography*, 118. https://doi.org/10.1016/j.dsr2.2015.02.009
Buchwald, C., Santoro, A. E., McIlvin, M. R., & Casciotti, K. L. (2012). Oxygen isotopic composition of nitrate and nitrite produced by nitrifying cocultures and natural marine assemblages. *Limnology and Oceanography*, *57*(5), 1361–1375. https://doi.org/10.4319/lo.2012.57.5.1361
Butterworth, B. J., & Miller, S. D. (2016). Air-sea exchange of carbon dioxide in the Southern Ocean and Antarctic marginal ice zone. *Geophysical Research Letters*, *43*, 7223–7230. https://doi.org/10.1002/2016GL069581
Carmack, E. C., Macdonald, R. W., & Jasper, S. (2004). Phytoplankton productivity on the Canadian Shelf of the Beaufort Sea. *Marine Ecology Progress Series*, *277*, 37–50. https://doi.org/10.3354/meps277037
Carpenter, J. H. (1965). The Chesapeake Bay Institute Techique for the Winker dissolved oxygen method. *Limnology and Oceanography*, *10*(1), 141–143. https://doi.org/10.4319/lo.1965.10.1.0141
Casciotti, K. L., Sigman, D. M., Hastings, M. G., Böhlke, J. K., & Hilkert, A. (2002). Measurement of the oxygen isotopic composition of nitrate in seawater and freshwater using the denitrifier method. *Analytical Chemistry*, *74*(19), 4905–4912. https://doi.org/10.1021/ac020113w
Casciotti, K. L., Trull, T. W., Glover, D. M., & Davies, D. (2008). Constraints on nitrogen cycling at the subtropical North Pacific Station ALOHA from isotopic measurements of nitrate and particulate nitrogen. *Deep-Sea Research Part II: Topical Studies in Oceanography*, *55*(14–15), 1661–1672. https://doi.org/10.1016/j.dsr2.2008.04.017
Chang, B. X., & Devol, A. H. (2009). Seasonal and spatial patterns of sedimentary denitrification rates in the Chukchi Sea. *Deep-Sea Research Part II: Topical Studies in Oceanography*, *56*(17), 1339–1350. https://doi.org/10.1016/j.dsr2.2008.10.024
Coachman, L. K., & Barnes, C. A. (1961). The contribution of Bering Sea Water to the Arctic Ocean. *Arctic*, *14*(3), 147–161. https://doi.org/10.14430/arctic3670
Coachman, L. K., Aagaard, K., & Tripp, R. B. (1975). *Bering Strait: The regional physical oceanography*. Seattle: University of Washington Press.
Comiso, J. C. (2011). Large decadal decline of the Arctic multiyear ice cover. *Journal of Climate*, *25*(4), 1176–1193. https://doi.org/10.1175/JCLI-D-11-00113.1
Cooper, L. W., Whitledge, T. E., Grebmeier, J. M., & Weingartner, T. (1997). The nutrient, salinity, and stable oxygen isotope composition of Bering and Chukchi Seas waters in and near the Bering Strait. *Journal of Geophysical Research*, *102*(C6), 12563–12573. https://doi.org/10.1029/97JC00015
Corlett, W. B., & Pickart, R. S. (2017). The Chukchi slope current. *Progress in Oceanography*, *153*, 50–65. https://doi.org/10.1016/j.pocean.2017.04.005
Dmitrenko, I. A., Kirillov, S. A., Ivanov, V. V., Rudels, B., Serra, N., & Koldunov, N. V. (2012). Modified halocline water over the Laptev Sea continental margin: Historical data analysis. *Journal of Climate*, *25*(16), 5556–5565. https://doi.org/10.1175/JCLI-D-11-00336.1
Epstein, S., & Mayeda, T. (1953). Variation of O18 content of waters from natural sources. *Geochimica et Cosmochimica Acta*, *4*(5), 213–224. https://doi.org/10.1016/0016-7037(53)90051-9
Falkner, K. K., Steele, M., Woodgate, R. A., Swift, J. H., Aagaard, K., & Morison, J. (2005). Dissolved oxygen extrema in the Arctic Ocean halocline from the North Pole to the Lincoln Sea. *Deep-Sea Research Part I: Oceanographic Research Papers*, *52*(7), 1138–1154. https://doi.org/10.1016/j.dsr.2005.01.007

Fripiat, F., Declercq, M., Anderson, L. G., Bruchert, V., Deman, F., Fonseca-Batista, D., et al. (2018). Influence of the bordering shelves on nutrient distribution in the Arctic halocline inferred from water column nitrate isotopes. *Limnology and Oceanography*. https://doi.org/10.1002/lno.10930

Furey, P. W. (1996). The large-scale surface wind field over the Western Arctic Ocean, 1981–1993. University of Alaska, Fairbanks.

Galley, R. J., Else, B. G. T., Prinsenberg, S. J., Babb, D., & Barber, D. G. (2013). Sea ice concentration, extent, age, motion and thickness in regions of proposed offshore oil and gas development near the Mackenzie Delta: Canadian Beaufort Sea. *Arctic*, *66*(1), 105–116.

Gonfiantini, R., Stichler, W., & Rozanski, K. (1995). Reference and intercomparison materials distributed by the International Atomic Energy Agency for stable isotope measurements. International Atomic Energy Agency, Vienna (Austria). Isotope Hydrology Sec. (165 pp.). IAEA-TECDOC-825.

Gong, D., & Pickart, R. S. (2015). Summertime circulation in the eastern Chukchi Sea. *Deep-Sea Research Part II: Topical Studies in Oceanography*, *118*, 18–31. https://doi.org/10.1016/j.dsr2.2015.02.006

Gordon, L. I., Jennings, J. C., Ross, A. A., & Krest, J. M. (1992). A suggested protocol for continuous flow automated analysis of seawater nutrients in the WOCE hydrographic program and the Joint Global Ocean Fluxes Study.

Granger, J., Prokopenko, M. G., Mordy, C. W., & Sigman, D. M. (2013). The proportion of remineralized nitrate on the ice-covered eastern Bering Sea shelf evidenced from the oxygen isotope ratios of nitrate. *Global Biogeochemical Cycles*, *27*, 962–971. https://doi.org/10.1002/gbc.20075

Granger, J., Prokopenko, M. G., Sigman, D. M., Mordy, C. W., Morse, Z. M., Morales, L. V., et al. (2011). Coupled nitrification-denitrification in sediment of the eastern Bering Sea shelf leads to ^{15}N enrichment of fixed N in shelf waters. *Journal of Geophysical Research*, *116*, C11006. https://doi.org/10.1029/2010JC006751

Granger, J., & Sigman, D. M. (2009). Removal of nitrite with sulfamic acid for nitrate N and O isotope analysis with the denitrifier method. *Rapid Communications in Mass Spectrometry*, *23*(23), 3753–3762. https://doi.org/10.1002/rcm.4307

Granger, J., Sigman, D. M., Lehmann, M. F., & Tortell, P. D. (2008). Nitrogen and oxygen isotope fractionation during dissimilatory nitrate reduction by denitrifying bacteria. *Limnology and Oceanography*, *53*(6), 2533–2545. https://doi.org/10.4319/lo.2008.53.6.2533

Granger, J., Sigman, D. M., Needoba, J. A., & Harrison, P. J. (2004). Coupled nitrogen and oxygen isotope fractionation of nitrate during assimilation by cultures of marine phytoplankton. *Limnology and Oceanography*, *49*(5), 1763–1773. https://doi.org/10.4319/lo.2004.49.5.1763

Grasshoff, K., Ehrhardt, M., & Kremling, K. (1983). Methods of seawater analysis. In *Verla Chemie* (237 pp.). Weinheim: Deutsche Bibliothek Cataloguing-in-Publication Data.

Gruber, N., & Sarmiento, J. L. (1997). Global patterns of marine nitrogen fixation and denitrification. *Global Biogeochemical Cycles*, *11*(2), 235–266. https://doi.org/10.1029/97GB00077

IPCC (2014). Climate Change 2014: Synthesis Report. In Core Writing Team, R. K. Pachauri, & L. A. Meyer (Eds.), *Contribution of Working Groups I, II and III to the Fifth Assessment Report of the Intergovernmental Panel on Climate Change* (p. 151). Geneva, Switzerland: IPCC.

Jackson, J. M., Allen, S. E., McLaughlin, F. A., Woodgate, R. A., & Carmack, E. C. (2011). Changes to the near-surface waters in the Canada Basin, Arctic Ocean from 1993–2009: A basin in transition. *Journal of Geophysical Research*, *116*, C10008. https://doi.org/10.1029/2011JC007069

Jackson, J. M., Carmack, E. C., McLaughlin, F. A., Allen, S. E., & Ingram, R. G. (2010). Identification, characterization, and change of the near-surface temperature maximum in the Canada Basin, 1993–2008. *Journal of Geophysical Research*, *115*, C05021. https://doi.org/10.1029/2009JC005265

James, M., Julienne, S., Charles, F., & William, E. (2011). Distribution and trends in Arctic Sea ice age through spring 2011. *Geophysical Research Letters*, *38*, L13502. https://doi.org/10.1029/2011GL047735

Jones, E. P., Anderson, L. G., & Swift, J. H. (1998). Distribution of Atlantic and Pacific waters in the upper Arctic Ocean: Implications for circulation. *Geophysical Research Letters*, *25*(6), 765–768. https://doi.org/10.1029/98GL00464

Jones, E. P., Anderson, L. G., & Wallace, D. W. R. (1991). Tracers of near-surface, halocline and deep waters in the Arctic Ocean: Implications for circulation. *Journal of Marine Systems*, *2*(1–2), 241–255. https://doi.org/10.1016/0924-7963(91)90027-R

Jones, E. P., & Anderson, L. G. G. (1986). On the origin of the chemical properties of the Arctic Ocean halocline. *Journal of Geophysical Research*, *91*(C9), 10759. https://doi.org/10.1029/JC091iC09p10759

Kinney, P., Arhelger, M. E., Burrell, D., & C. (1970). Chemical characteristics of water masses in the Amerasian Basin of the Arctic Ocean. *Journal of Geophysical Research*, *75*(21), 4097–4104. https://doi.org/10.1029/JC075i021p04097

Lansard, B., Mucci, A., Miller, L. A., MacDonald, R. W., & Gratton, Y. (2012). Seasonal variability of water mass distribution in the southeastern Beaufort Sea determined by total alkalinity and d^{18}O. *Journal of Geophysical Research*, *117*, C03003. https://doi.org/10.1029/2011JC007299

Le Fouest, V., Zakardjian, B., Xie, H., Raimbault, P., Joux, F., & Babin, M. (2013). Modeling plankton ecosystem functioning and nitrogen fluxes in the oligotrophic waters of the Beaufort Sea, Arctic Ocean: A focus on light-driven processes. *Biogeosciences*, *10*(7), 4785–4800. https://doi.org/10.5194/bg-10-4785-2013

Lehmann, M. F., Sigman, D. M., & Berelson, W. M. (2004). Coupling the $^{15}N/^{14}N$ and $^{18}O/^{16}O$ of nitrate as a constraint on benthic nitrogen cycling. *Marine Chemistry*, *88*(1–2), 1–20. https://doi.org/10.1016/j.marchem.2004.02.001

Lehmann, M. F., Sigman, D. M., McCorkle, D. C., Brunelle, B. G., Hoffmann, S., Kienast, M., et al. (2005). Origin of the deep Bering Sea nitrate deficit: Constraints from the nitrogen and oxygen isotopic composition of water column nitrate and benthic nitrate fluxes. *Global Biogeochemical Cycles*, *19*, GB4005. https://doi.org/10.1029/2005GB002508

Lehmann, M. F., Sigman, D. M., McCorkle, D. C., Granger, J., Hoffmann, S., Cane, G., & Brunelle, B. G. (2007). The distribution of nitrate $^{15}N/^{14}N$ in marine sediments and the impact of benthic nitrogen loss on the isotopic composition of oceanic nitrate. *Geochimica et Cosmochimica Acta*, *71*(22), 5384–5404. https://doi.org/10.1016/j.gca.2007.07.025

Linders, J., Pickart, R. S., Björk, G., & Moore, G. W. K. (2017). On the nature and origin of water masses in Herald Canyon, Chukchi Sea: Synoptic surveys in summer 2004, 2008, and 2009. *Progress in Oceanography*, *159*, 99–114. https://doi.org/10.1016/j.pocean.2017.09.005

Lowry, K. E., Pickart, R. S., Mills, M. M., Brown, Z. W., van Dijken, G. L., Bates, N. R., & Arrigo, K. R. (2015). The influence of winter water on phytoplankton blooms in the Chukchi Sea. *Deep-Sea Research Part II: Topical Studies in Oceanography*, *118*, 53–72. https://doi.org/10.1016/j.dsr2.2015.06.006

Macdonald, R. W., & Carmack, E. C. (1991). Age of Canada Basin deep waters: A way to estimate primary production for the Arctic Ocean. *Science*, *254*(5036), 1348–1350. https://doi.org/10.1126/science.254.5036.1348

Mantoura, R. F. C., & Woodward, E. M. S. (1983). Conservative behaviour of riverine dissolved organic carbon in the Severn Estuary: Chemical and geochemical implications. *Geochimica et Cosmochimica Acta*, *47*(7), 1293–1309. https://doi.org/10.1016/0016-7037(83)90069-8

Marconi, D., Weigand, M. A., Rafter, P. A., McIlvin, M. R., Forbes, M., Casciotti, K. L., & Sigman, D. M. (2015). Nitrate isotope distributions on the US GEOTRACES North Atlantic cross-basin section: Signals of polar nitrate sources and low latitude nitrogen cycling. *Marine Chemistry*, *177*. https://doi.org/10.1016/j.marchem.2015.06.007

Mariotti, A., Germon, J. C., Hubert, P., Kaiser, P., Letolle, R., Tardieux, A., & Tardieux, P. (1981). Experimental determination of nitrogen kinetic isotope fractionation: Some principles; illustration for the denitrification and nitrification processes. *Plant and Soil*, *62*(3), 413–430. https://doi.org/10.1007/BF02374138

Marnela, M., Rudels, B., Goszczko, I., Beszczynska-Möller, A., & Schauer, U. (2016). Fram Strait and Greenland Sea transports, water masses, and water mass transformations 1999–2010 (and beyond). *Journal of Geophysical Research: Oceans*, *121*, 2314–2346. https://doi.org/10.1002/2015JC011312

McIlvin, M. R., & Casciotti, K. L. (2011). Technical updates to the bacterial method for nitrate isotopic analyses. *Analytical Chemistry*, *83*(5), 1850–1856. https://doi.org/10.1021/ac1028984

McLaughlin, F., Carmack, E., Proshutinsky, A., Krishfield, R. A., Guay, C., Yamamoto-Kawai, M., et al. (2011). The rapid response of the Canada basin to climate forcing from bellwether to alarm bells. *Oceanography*, *24*(3), 146–159. https://doi.org/10.5670/oceanog.2011.66

McLaughlin, F., & Carmack, E. C. (2010). Deepening of the nutricline and chlorophyll maximum in the Canada Basin interior, 2003–2009. *Geophysical Research Letters*, *37*, L24602. https://doi.org/10.1029/2010GL045459

Melling, H., Lake, R. A., Topham, D. R., & Fissel, D. B. (1984). Oceanic thermal structure in the western Canadian Arctic. *Continental Shelf Research*, *3*(3), 233–258. https://doi.org/10.1016/0278-4343(84)90010-4

Melling, H., & Moore, R. M. (1995). Modification of halocline source waters during freezing on the Beaufort Sea shelf: Evidence from oxygen isotopes and dissolved nutrients. *Continental Shelf Research*, *15*(1), 89–113. https://doi.org/10.1016/0278-4343(94)P1814-R

Mills, M. M., Brown, Z. W., Lowry, K. E., van Dijken, G. L., Becker, S., Pal, S., et al. (2015). Impacts of low phytoplankton NO_3^-: PO_4^{3-} Utilization ratios over the Chukchi Shelf. *Arctic Ocean. Deep-Sea Research Part II: Topical Studies in Oceanography*, 118. https://doi.org/10.1016/j.dsr2.2015.02.007

Moore, R. M., Lowings, M. G., & Tan, F. (1983). Geochemical profiles in the central Arctic Ocean: Their relation to freezing and shallow circulation. *Journal of Geophysical Research*, *88*(C4), 2667–2674. https://doi.org/10.1029/JC088iC04p02667

Moore, R. M., & Smith, J. N. (1986). Disequilibria between ^{226}Ra, ^{210}Pb and ^{210}Po in the Arctic Ocean and the implications for chemical modification of the Pacific water inflow. *Earth and Planetary Science Letters*, *77*(3–4), 285–292. https://doi.org/10.1016/0012-821X(86)90140-8

Morales, L. V., Granger, J., Chang, B. X., Prokopenko, M. G., Plessen, B., Gradinger, R., & Sigman, D. M. (2014). Elevated 15N/14N in particulate organic matter, zooplankton, and diatom frustule-bound nitrogen in the ice-covered water column of the Bering Sea eastern shelf. *Deep-Sea Research Part II: Topical Studies in Oceanography*, 109. https://doi.org/10.1016/j.dsr2.2014.05.008

Morison, J., Kwok, R., Peralta-Ferriz, C., Alkire, M., Rigor, I., Andersen, R., & Steele, M. (2012). Changing Arctic Ocean freshwater pathways. *Nature*, *481*(7379), 66–70. https://doi.org/10.1038/nature10705

Mountain, D. G., Coachman, L. K., & Aagaard, K. (1976). On the flow through Barrow Canyon. *Journal of Physical Oceanography*, *6*(4), 461–470. https://doi.org/10.1175/1520-0485(1976)006<0461:OTFTBC>2.0.CO;2

Münchow, A., & Carmack, E. C. (1997). Synoptic flow and density observations near an arctic shelf break. *Journal of Physical Oceanography*, *27*(7), 1402–1419. https://doi.org/10.1175/1520-0485(1997)027<1402:SFADON>2.0.CO;2

Nishino, S., Kikuchi, T., Fujiwara, A., Hirawake, T., & Aoyama, M. (2016). Water mass characteristics and their temporal changes in a biological hotspot in the southern Chukchi Sea. *Biogeosciences*, *13*(8), 2563–2578. https://doi.org/10.5194/bg-13-2563-2016

Paquette, R. G., & Bourke, R. H. (1974). Observations on the coastal current of Arctic Alaska. *Journal of Marine Research*, *32*(2), 195–207.

Perovich, D. K., & Richter-Menge, J. A. (2009). Loss of sea ice in the Arctic. *Annual Review of Marine Science*, *1*(1), 417–441. https://doi.org/10.1146/annurev.marine.010908.163805

Pickart, R. S., Weingartner, T. J., Pratt, L. J., Zimmermann, S., & Torres, D. J. (2005). Flow of winter-transformed Pacific water into the Western Arctic. *Deep-Sea Research Part II: Topical Studies in Oceanography*, *52*(24–26), 3175–3198. https://doi.org/10.1016/j.dsr2.2005.10.009

Pisareva, M. N., Pickart, R. S., Iken, K., Ershova, E. A., Grebmeier, J. M., Cooper, L. W., et al. (2015). The relationship between patterns of benthic fauna and zooplankton in the Chukchi Sea and physical forcing. *Oceanography*, *28*(3), 68–83. https://doi.org/10.5670/oceanog.2015.58

Pnyushkov, A. V., Polyakov, I. V., Ivanov, V. V., Aksenov, Y., Coward, A. C., Janout, M., & Rabe, B. (2015). Structure and variability of the boundary current in the Eurasian Basin of the Arctic Ocean. *Deep Sea Research Part I: Oceanographic Research Papers*, *101*, 80–97. https://doi.org/10.1016/j.dsr.2015.03.001

Rafter, P. A., Difiore, P. J., & Sigman, D. M. (2013). Coupled nitrate nitrogen and oxygen isotopes and organic matter remineralization in the Southern and Pacific Oceans. *Journal of Geophysical Research: Oceans*, *118*, 4781–4794. https://doi.org/10.1002/jgrc.20316

Redfield, A. C. (1934). On the proportion of organic derivates in sea water and their relation to the composition of plankton. In *James Johnstone Memorial Volume* (pp. 177–192). Liverpool: Liverpool University Press.

Redfield, A. C. (1958). The biological control of chemical factors in the environment. *American Scientist*, *46*(3), 205–221.

Redfield, A. C., Ketchum, B. H., & Richard, F. A. (1963). The influence of organisms on the composition of seawater. In M. N. Hill (Ed.), *The sea* (Vol. 2, pp. 26–77). New York, New York: Wiley-Interscience.

Roach, A. T., Aagaard, K., Pease, C. H., Salo, S. A., Weingartner, T., Pavlov, V., & Kulakov, M. (1995). Direct measurements of transport and water properties through the Bering Strait. *Journal of Geophysical Research*, *100*(C9), 18443. https://doi.org/10.1029/95JC01673

Rudels, B. (1995). The thermohaline circulation of the Arctic Ocean and the Greenland Sea. *Philosophical Transactions of the Royal Society of London A*, *352*(1699), 287–299.

Rudels, B. (2010). Constraints on exchanges in the Arctic Mediterranean—Do they exist and can they be of use? *Tellus Series A: Dynamic Meteorology and Oceanography*, *62*(2), 109–122. https://doi.org/10.1111/j.1600-0870.2009.00425.x

Rudels, B., Anderson, L. G., & Jones, E. P. (1996). Formation and evolution of the surface mixed layer and halocline of the Arctic Ocean. *Journal of Geophysical Research*, *101*(C4), 8807–8821. https://doi.org/10.1029/96JC00143

Rudels, B., Jones, E. P., Schauer, U., & Eriksson, P. (2004). Atlantic sources of the Arctic Ocean surface and halocline waters. *Polar Research*, *23*(2), 181–208. https://doi.org/10.3402/polar.v23i2.6278

Schlitzer, R. (2016). Ocean data view.

Schlosser, P., Kromer, B., Ekwurzel, B., Bönisch, G., McNichol, A., Schneider, R., et al. (1997). The first trans-Arctic 14C section: Comparison of the mean ages of the deep waters in the Eurasian and Canadian basins of the Arctic Ocean. *Nuclear Instruments and Methods in Physics Research Section B: Beam Interactions with Materials and Atoms*, *123*(1–4), 431–437. https://doi.org/10.1016/S0168-583X(96)00677-5

Serreze, M. C., Barrett, A. P., Slater, A. G., Woodgate, R. A., Aagaard, K., Lammers, R. B., et al. (2006). The large-scale freshwater cycle of the Arctic. *Journal of Geophysical Research*, *111*, C11010. https://doi.org/10.1029/2005JC003424

Shimada, K., Carmack, E. C., Hatakeyama, K., & Takizawa, T. (2001). Varieties of shallow temperature maximum waters in the Western Canadian Basin of the Arctic Ocean. *Geophysical Research Letters*, *28*(18), 3441–3444. https://doi.org/10.1029/2001GL013168

Shimada, K., Kamoshida, T., Itoh, M., Nishino, S., Carmack, E., McLaughlin, F., et al. (2006). Pacific Ocean inflow: Influence on catastrophic reduction of sea ice cover in the Arctic Ocean. *Geophysical Research Letters*, *33*, L08605. https://doi.org/10.1029/2005GL025624

Sigman, D. M., Casciotti, K. L., Andreani, M., Barford, C., Galanter, M., & Böhlke, J. K. (2001). A bacterial method for the nitrogen isotopic analysis of nitrate in seawater and freshwater. *Analytical Chemistry*, *73*(17), 4145–4153. https://doi.org/10.1021/ac010088e

Sigman, D. M., DiFiore, P. J., Hain, M. P., Deutsch, C., Wang, Y., Karl, D. M., et al. (2009). The dual isotopes of deep nitrate as a constraint on the cycle and budget of oceanic fixed nitrogen. *Deep-Sea Research Part I: Oceanographic Research Papers*, *56*(9). https://doi.org/10.1016/j.dsr.2009.04.007

Sigman, D. M., Granger, J., DiFiore, P. J. J., Lehmann, M. M. M., Ho, R., Cane, G., & van Geen, A. (2005). Coupled nitrogen and oxygen isotope measurements of nitrate along the eastern North Pacific margin. *Global Biogeochemical Cycles*, *19*, GB4022. https://doi.org/10.1029/2005GB002458

Spall, M. A., Pickart, R. S., Fratantoni, P. S., & Plueddemann, A. J. (2008). Western Arctic shelfbreak eddies: Formation and transport. *Journal of Physical Oceanography*, *38*(8), 1644–1668. https://doi.org/10.1175/2007JPO3829.1

Steele, M., Morison, J., Ermold, W., Rigor, I., Ortmeyer, M., & Shimada, K. (2004). Circulation of summer Pacific halocline water in the Arctic Ocean. *Journal of Geophysical Research*, *109*, C02027. https://doi.org/10.1029/2003JC002009

Swift, J. H., Jones, E. P., Aagaard, K., Carmack, E. C., Hingston, M., Macdonald, R. W., et al. (1997). Waters of the Makarov and Canada basins. *Deep-Sea Research Part II: Topical Studies in Oceanography*, *44*(8), 1503–1529. https://doi.org/10.1016/S0967-0645(97)00055-6

Timmermans, M.-L., & Garrett, C. (2006). Evolution of the deep water in the Canadian Basin in the Arctic Ocean. *Journal of Physical Oceanography*, *36*(5), 866–874. https://doi.org/10.1175/JPO2906.1

Timmermans, M.-L., Garrett, C., & Carmack, E. (2003). The thermohaline structure and evolution of the deep waters in the Canada Basin, Arctic Ocean. *Deep-Sea Research Part I: Oceanographic Research Papers*, *50*(10–11), 1305–1321. https://doi.org/10.1016/S0967-0637(03)00125-0

Timmermans, M.-L., Proshutinsky, A., Golubeva, E., Jackson, J. M., Krishfield, R., McCall, M., et al. (2014). Mechanisms of Pacific summer water variability in the Arctic's Central Canada Basin. *Journal of Geophysical Research: Oceans*, *119*, 7523–7548. https://doi.org/10.1002/2014JC010273

Toole, J. M., Timmermans, M.-L., Perovich, D. K., Krishfield, R. A., Proshutinsky, A., & Richter-Menge, J. A. (2010). Influences of the ocean surface mixed layer and thermohaline stratification on Arctic Sea ice in the central Canada Basin. *Journal of Geophysical Research*, *115*, C10018. https://doi.org/10.1029/2009JC005660

Tremblay, J.-É., Anderson, L. G., Matrai, P., Coupel, P., Bélanger, S., Michel, C., & Reigstad, M. (2015). Global and regional drivers of nutrient supply, primary production and CO_2 drawdown in the changing Arctic Ocean. *Progress in Oceanography*, *139*, 171–196. https://doi.org/10.1016/j.pocean.2015.08.009

Wallace, D. W. R., Moore, R. M., & Jones, E. P. (1987). Ventilation of the Arctic Ocean cold halocline: Rates of diapycnal and isopycnal transport, oxygen utilization and primary production inferred using chlorofluoromethane distributions. *Deep Sea Research Part A, Oceanographic Research Papers*, *34*(12), 1957–1979. https://doi.org/10.1016/0198-0149(87)90093-8

Walsh, J. J., McRoy, C. P., Coachman, L. K., Goering, J. J., Nihoul, J. J., Whitledge, T. E., et al. (1989). Carbon and nitrogen cycling within the Bering/Chukchi Seas: Source regions for organic matter effecting AOU demands of the Arctic Ocean. *Progress in Oceanography*, *22*(4), 277–359. https://doi.org/10.1016/0079-6611(89)90006-2

Wang, J., Cota, G. F., & Comiso, J. C. (2005). Phytoplankton in the Beaufort and Chukchi Seas: Distribution, dynamics, and environmental forcing. *Deep-Sea Research Part II: Topical Studies in Oceanography*, *52*(24–26), 3355–3368. https://doi.org/10.1016/j.dsr2.2005.10.014

Watson, A. J., Messias, M.-J., Fogelqvist, E., Van Scoy, K. A., Johannessen, T., Oliver, K. I. C., et al. (1999). Mixing and convection in the Greenland Sea from a tracer-release experiment. *Nature*, *401*(6756), 902–904. https://doi.org/10.1038/44807

Weigand, M. A., Foriel, J., Barnett, B., Oleynik, S., & Sigman, D. M. (2016). Updates to instrumentation and protocols for isotopic analysis of nitrate by the denitrifier method. *Rapid Communications in Mass Spectrometry*, *30*(12), 1365–1383. https://doi.org/10.1002/rcm.7570

Weingartner, T. J., Cavalieri, D. J., Aagaard, K., & Sasaki, Y. (1998). Circulation, dense water formation, and outflow on the northeast Chukchi shelf. *Journal of Geophysical Research*, *103*(C4), 7647–7661. https://doi.org/10.1029/98JC00374

Weingartner, T. J., Potter, R. A., Stoudt, C. A., Dobbins, E. L., Statscewich, H., Winsor, P. R., et al. (2017). Transport and thermohaline variability in Barrow Canyon on the Northeastern Chukchi Sea Shelf. *Journal of Geophysical Research: Oceans*, *122*, 3565–3585. https://doi.org/10.1002/2016JC012636

Weiss, R. F. (1970). The solubility of nitrogen, oxygen and argon in water and seawater. *Deep-Sea Research and Oceanographic Abstracts*, *17*(4), 721–735. https://doi.org/10.1016/0011-7471(70)90037-9

Whitledge, T. E., Reeburgh, W. S., & Walsh, J. J. (1986). Seasonal inorganic nitrogen distributions and dynamics in the southeastern Bering Sea. *Continental Shelf Research*, *5*(1–2), 109–132. https://doi.org/10.1016/0278-4343(86)90012-9

Woodgate, R. A., Aagaard, K., Swift, J. H., Falkner, K. K., Smethie, W. M., & Smethie, W. M. Jr. (2005). Pacific ventilation of the Arctic Ocean's lower halocline by upwelling and diapycnal mixing over the continental margin. *Geophysical Research Letters*, *32*, L18609. https://doi.org/10.1029/2005GL023999

Yamamoto-Kawai, M., Carmack, E., & McLaughlin, F. (2006). Nitrogen balance and Arctic throughflow. *Nature*, *443*(7107), 43. https://doi.org/10.1038/443043a

Yamamoto-Kawai, M., McLaughlin, F. A., Carmack, E. C., Nishino, S., Shimada, K., & Kurita, N. (2009). Surface freshening of the Canada Basin, 2003–2007: River runoff versus sea ice meltwater. *Journal of Geophysical Research*, *114*, C00A05. https://doi.org/10.1029/2008JC005000

Erratum

In the originally published version of this article, Figure 1 did not render correctly and Equation 1 contained typographical errors. This has since been corrected, and this version may be considered the authoritative version of record.